

Understanding the role of structural disorder on spin polarization in CeMnNi₄ using XAFS

Debdutta Lahiri,^{1,*} S. Khalid,² P. Modak,¹ Pratap Raychaudhuri,³ S. K. Dhar,³ and Surinder M. Sharma¹

¹High Pressure and Synchrotron Radiation Physics Division, Bhabha Atomic Research Centre, Mumbai 400085, India

²National Synchrotron Light Source, Brookhaven National Laboratory, Upton, New York 11973, USA

³Department of Condensed Matter Physics and Materials Science, Tata Institute of Fundamental Research, Colaba, Mumbai 400005, India

(Received 3 February 2010; revised manuscript received 30 July 2010; published 14 October 2010)

The role of disorder on ferromagnetism has generally been detrimental. We show how Mn-Ni antisite disorder enhances polarization in CeMnNi₄. The disorder is determined to be 6% by x-ray absorption fine structure. The electronic structure of pure CeMnNi₄ is pseudo-half-metallic. Site exchange alters the near neighbor bond parameters and modifies the density of states favorably, increasing the polarization (obtained by first-principles calculations) from 13 to 47% (experimental ~66%).

DOI: [10.1103/PhysRevB.82.134424](https://doi.org/10.1103/PhysRevB.82.134424)

PACS number(s): 85.75.-d, 61.05.aj

I. INTRODUCTION

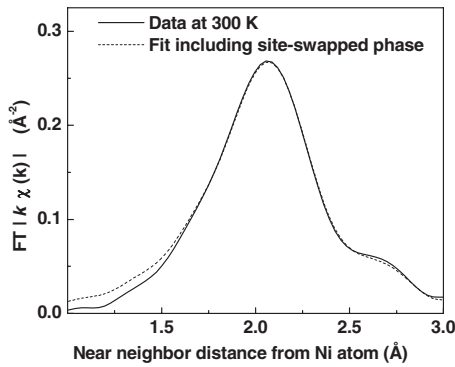
A huge thrust in contemporary scientific research is on the new paradigm of electronics (viz., spintronics), utilizing the spin degree of freedom of the electron.¹ This additional degree of freedom promises fundamentally new advances in device industry in terms of nonvolatility, increased data processing speed, decreased electric power consumption, and increased integration densities. The success of spintronics is conditional upon detectable spin polarization at room temperature. Though several materials have been theoretically predicted for large polarization,² a major bottleneck for their practical realization is nanoscale coherence length of spin current, which makes them ultrasensitive to the existence of structural disorder or defects. Therefore, the (largely detrimental) role of structural disorder on polarization has been well addressed problem in spintronic science.³ Interestingly, a few recent experiments defied this conventional and over-emphasized detrimental notion of disorder by demonstrating disorder-induced ferromagnetism.^{4,5} This could have interesting implications for the development of spintronic materials that had been long toiling on minimizing defects. The formation of defects being intrinsic and thermodynamically favored, this would be considerably easier than the conventional scheme (by reducing defects) of developing spintronic materials. Further, new functionalities employing disorder can be conceived.⁵

The interest in the present work was motivated by the recently (experimental) reported enhancement in polarization (~66%) in CeMnNi₄ (Ref. 6) ($T_c=140$ K), compared to the theoretically predicted value of ~20% for the pure compound.⁷ The unusual electronic structure of this material emulates *near* half-metallic⁸ character, marked by a pseudogap at the Fermi level for both the spin channels. Antisite disorder (~5–10 %) is ironically favored in this material by identical atomic radii of the component metals Mn-Ni. Earlier work on half metals reports the detrimental role of such antisite disorder on polarization.^{9,10} The object of this paper is probing the degree of antisite disorder (predictably Mn-Ni) in this material using x-ray absorption fine structure (XAFS) (described later) and recalculating polarization (electronic structure) on the basis of the XAFS-

derived bond parameters. Neutron diffraction, though indicated large disorder for Mn atom, could not conclusively identify the origin of this disorder.¹¹ The uncertainties in the neutron-diffraction results entail from the large number of variables and could be significantly reduced by employing an element-specific technique, such as XAFS.¹² XAFS is the modulation in the absorption spectrum of an atom due to the presence of neighboring atoms. By analyzing XAFS, one can obtain detailed information on the species, bond length (R), coordination (N), and disorder [Debye-Waller factor (DWF)] of the neighboring atoms. The abundance of antisite disorder may subsequently be derived from the coordination information. Ni K edge (rather than Mn K edge) has been excited to extract the above information. Since Ce L_1 edge (6.549 keV) closely follows the Mn K edge (6.5399 keV), it would superimpose on the latter, thus rendering the Mn K -edge XAFS unusable. Our analysis of the data clearly resolves (i) the existence of Mn-Ni antisite defects; (ii) their abundance to be 6% (i.e., one site per supercell); (iii) the defect-induced disorder in bond-length distribution, and (iv) their thermal evolution. Revised electronic structure calculations, based on XAFS results, raised the polarization drastically to ~47% (closer to the experimental value).

II. EXPERIMENTAL DETAILS

The polycrystalline alloy was prepared by arc melting.¹³ The sample was sealed in an ampule and transported to the synchrotron facility. The sealed *ampule* (preserved in a *desiccator*) was broken inside glovebox, ~30–40 min prior to the XAFS measurements. The sample was ground (inside glovebox) to powder of particle size ~5 μm (Ref. 14) and uniformly pasted on tape for the XAFS experiments. The tape was taken out of the glovebox and promptly inserted into the two-stage closed cycle *displex* cryostat sample holder. The cryostat was pumped down. Temperature-dependent Ni K -edge XAFS data were collected in transmission mode at X18B¹⁵ bending magnet beamline, NSLS (USA). Si (111) monochromator was used to filter out the wavelengths and detuned to suppress the higher harmonics from the monochromator. The incident and transmitted beam intensities were measured with ionization chambers. The

FIG. 1. Fourier transform of XAFS data at Ni *K* edge.

data were processed using ATHENA.¹⁶ The persistence of XAFS oscillations up to $k=15 \text{ \AA}^{-1}$ confirms good crystalline quality of the sample. The structural parameters (bond length, coordination, and DWF) were obtained through the fits to the experimental data using the programs ATOMS, FEFF8, and FEFFIT.¹⁶ k^1 -weighted XAFS data, transformed over k range of $2.5\text{--}14 \text{ \AA}^{-1}$, are shown in Fig. 1. The electronic structure and static spin polarization were calculated using *ab initio* pseudopotential method based on density-functional theory as implemented in the VASP code.¹⁷

III. RESULTS AND DISCUSSIONS

A. XAFS analysis

Both structural models, viz., (i) pure crystalline phase (model I) and (ii) binary phase (model II) that includes site-exchanged fraction, were considered. CeMnNi_4 crystallizes in the $F\bar{4}3m$ group, with the atoms ideally positioned at Ce (0, 0, 0), Ni (0.625, 0.625, 0.625), and Mn (0.25, 0.25, 0.25).¹¹ The bond lengths for the pure phase were generated using the crystallographic structural parameters in the ATOMS program.¹⁶ The bond lengths corresponding to the site-

exchanged phase were generated by interchanging the Ni and Mn sites in the ATOMS file. The difference between the resulting bond parameters of the two phases is shown in Table I and the corresponding structures in Fig. 2. In Fig. 1, the first peak (2.05 \AA) of the data is contributed by Ni neighbors and its tail (small hump), between 2.5 and 3 \AA , by Ce and Mn neighbors (for ordered structure).¹⁸ k^1 -weighted data, transformed over k range of $2.5\text{--}14 \text{ \AA}^{-1}$, were fitted over the R range of $1.5\text{--}3 \text{ \AA}$. (The higher k weights deemphasized the hump and k^0 weight caused leakage from higher order peaks.) In order to reduce uncertainties, simultaneous fitting for data at all the temperatures was performed by constraining the coordination and bond-length variables to be common between temperatures and allowing only the Debye-Waller factors to vary.¹⁹ Multielectron excitation factor $S_0^2 (=0.9)$ in XAFS equation¹² was fixed from fitting data for Ni foil. The bond lengths attained crystallographic values and were, thereafter, fixed to those values to reduce uncertainties further. At first-hand fitting attempt, the coordination for Ni and Mn bonds resulted as approximately 4 each, which is markedly different from their respective ideal values (viz., $N_{\text{Ni}}=6$ and $N_{\text{Mn}}=3$). This is clear indication of deviation from pure structure. Fit constraining the coordination to the ideal values (i.e., model I) resulted in unphysical values for the Debye-Waller factors. For example, Ni-Ce bond disorder ($\sim 0.035 \text{ \AA}^2$ at room temperature) is found to be drastically larger than that for the Ni-Mn bond ($\sim 0.011 \text{ \AA}^2$), in sharp contrast to the physical situation (i.e., $\text{DWF}=0.035 \text{ \AA}^2$ is equivalent to practical nonexistence of the bond), theoretical prediction, and neutron-diffraction results.^{7,11}

The fit strategy using model II included a linear combination of the ordered and site-exchanged phases, the fraction (x) of antisite defect being the variable of interest (to quantify the abundance of antisite defect). The site exchange generates *inequivalent* sites for Ni, as shown in Table I. Setting 1 [fractionally $(1-x)$], the ideal Ni site, now has a modified environment with (i) $(6-\Delta N)$ Ni and (ΔN) Mn nearest neighbors ($\Delta N=6x$) at 2.45 \AA , (ii) three Ce neighbors at

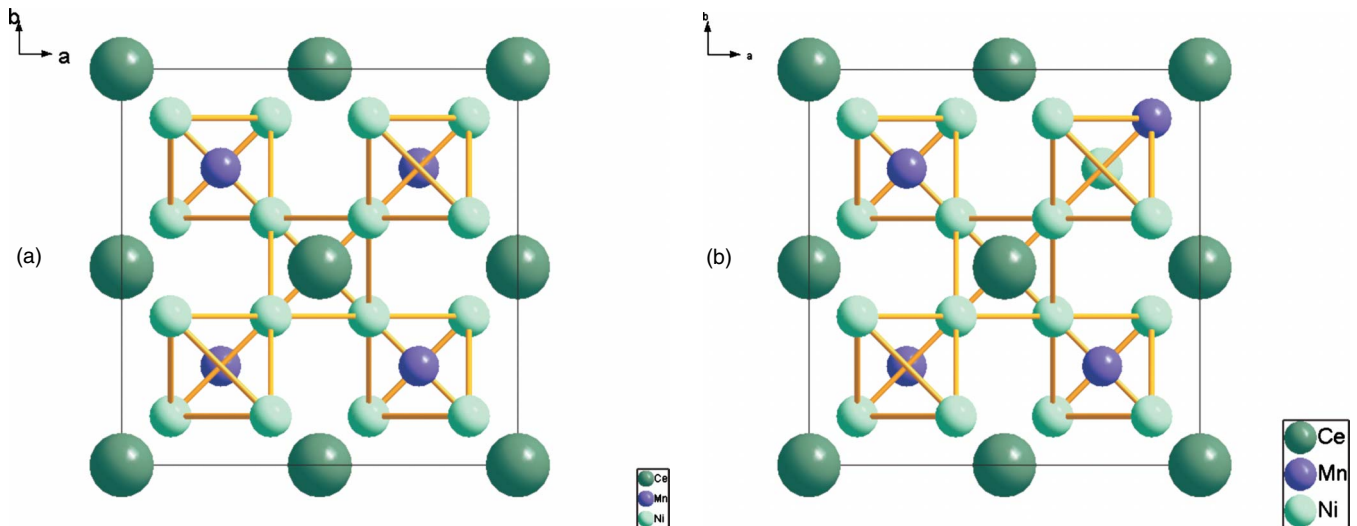
FIG. 2. (Color online) Crystal structure of CeMnNi_4 (a) ordered fcc structure and (b) simple-cubic supercell for site-exchanged structure.

TABLE I. The bond-length values for pure (site 1) and site-exchanged (site 2) phases of CeMnNi₄.

	Site 1 $R[N]$	Site 2 $R[N]$	N for mixed phase		Factors to be added for N_{av}	
Ni-Ni	2.45 Å (6)		[6(1-x)]		(1-x)	
Ni-Mn			[6x]			
Ni-Ce	2.88 Å (3)		3		(1-x)	
Ni-Mn	2.88 Å (3)	2.88 Å (12)	3-6x	6x	(1-x) (site 1)	x (site 2)
Ni-Ni			6x (site 1)	12-6x (site 2)		

2.88 Å, and (iii) (3- ΔN) Mn and (ΔN) Ni neighbors at 2.88 Å. Setting 2 (fractionally x), the exchanged site, has (12- ΔN) Ni and (ΔN) Mn neighbors at 2.88 Å. In Table I, the final coordination (N_{av}) is obtained by averaging over both sites (taking into account their respective abundances). These figures are reflected as coordination during actual fitting. N_{av} , the coordination for each scattering path in feffit.inp file, is set to be the corresponding product of columns 4 and 5 in Table I. From Table I, it is clear that any fraction x of antisite defect would reduce the nearest-neighbor Ni coordination by a factor of (1-x), which justifies the initially observed lower Ni coordination.

The fitting procedure was nontrivial since Mn and Ni, having closely spaced atomic numbers, have almost identical backscattering factors. This rendered Ni and Mn simultaneous scattering contributions to XAFS redundant. Nor could the Mn contribution be simply replaced by Ni (or its multiplicative factor). (The XAFS contribution by Ni is reproducible by 70% of that of Mn but for some modification in DWF.) The problem was efficiently addressed by first assuming Mn and Ni indistinguishable for fitting (i.e., no separate contribution included for Ni and Mn for the same bond length) and then, adding an uncertainty in estimation (by replacing the Ni with Mn and vice versa) to the best fit value. The best fit results (R factor=0.001), thus obtained, yielded $x=15\% \pm 3\%$. The quality of the fit is shown in Fig. 1. $x=15\%$ corresponds to $\Delta N \sim 1$ [$\Delta N=6x$], i.e., only one Ni-Mn antisite defect exists in every six unit cells. (The total number of Ni atoms in supercell being 16, $\Delta N \sim 1$ would amount to 6.25% antisite disorder per supercell.)

The coexistence of two structural phases is further confirmed by the thermal evolution of the DWF, as shown in Fig. 3. Close inspection of Fig. 3 (inset) reveals that the disorder ramps up fast until 160 K, followed by a relatively flat slope. It best represents a superposition of two Debye model of biphasic system. That Ni-Mn DWF is the largest is consistent with disorder in Mn sites (Ni-Mn antisite defect).

B. Theoretical calculations

We performed electronic structure calculations both for ordered (fcc) and site swapped structures using projector augmented wave pseudopotential. In case of ordered structure, starting with the experimental lattice constant (6.987 Å), we relaxed Ni positions using conjugate gradient optimizations. For the exchange-correlation terms we used generalized gradient approximations of Perdew-Burke-Ernzerhof.²⁰ We have selected kinetic-energy

cutoff as 368 eV and augmentation charge cutoff as 703 eV for the plane-wave basis set. In the pseudopotential, 3d and 4s states of transition-metal atoms are treated as valence states and 3p state as semicore states, whereas for Ce atoms 4f, 5d, and 6s states are considered as valence states and 5s, 5p states as semicore states. A $15 \times 15 \times 15$ Monkhorst-Pack k -point grid has been used for Brillouin-zone (BZ) sampling which yields 120 k points for the irreducible wedge of the BZ. To study the effect of site exchange between Mn and Ni atoms, we have employed a simple-cubic supercell which has 4 f.u. of CeMnNi₄ and interchanged one position (6.25%) between Mn and Ni atoms. To add bond-length disorder we have used the experimentally determined Ni-bond-length distributions and accordingly changed the Ni positions. For this simple-cubic supercell we have taken $10 \times 10 \times 10$ k -point grid for BZ sampling. The static spin polarization is defined as $P=[D\uparrow(E_F)-D\downarrow(E_F)]/[D\uparrow(E_F)+D\downarrow(E_F)]$, where $D\uparrow(E_F)$ and $D\downarrow(E_F)$ are the spin-up and spin-down densities of states (DOSs) at Fermi level, respectively. Our calculated magnetic moment for the ordered structure is $4.9\mu_B/\text{f.u.}$, which is in good agreement with earlier calculations⁷ and experimentally observed value. Our calculated total and site projected DOS for ordered structure is shown in Fig. 4. In total DOS, the Fermi level (E_F) is observed to lie on the local minimum for both the spin channels and correspondingly, the static spin polarization is only -13.2%, in agreement with the earlier calculations.⁷ From site projected DOSs we found that the Mn 3d electrons are mainly responsible for the magnetism in this compound. The Ce 4f states lie above E_F and hence no on-site Coulomb type potential is required for this level. The Ni 3d states are nearly equally populated for both the spin channels. Single site ex-

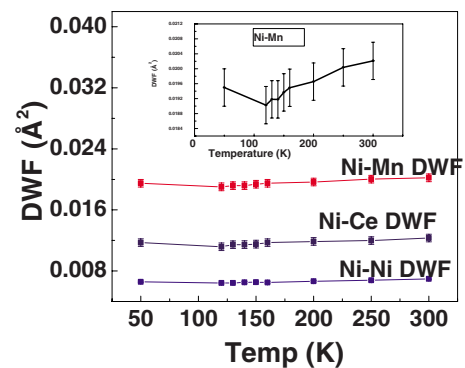


FIG. 3. (Color online) Debye-Waller factors for various bonds of CeMnNi₄ as a function of temperature (as deduced from our EXAFS data). Shown in inset is the evolution of Ni-Mn bond.

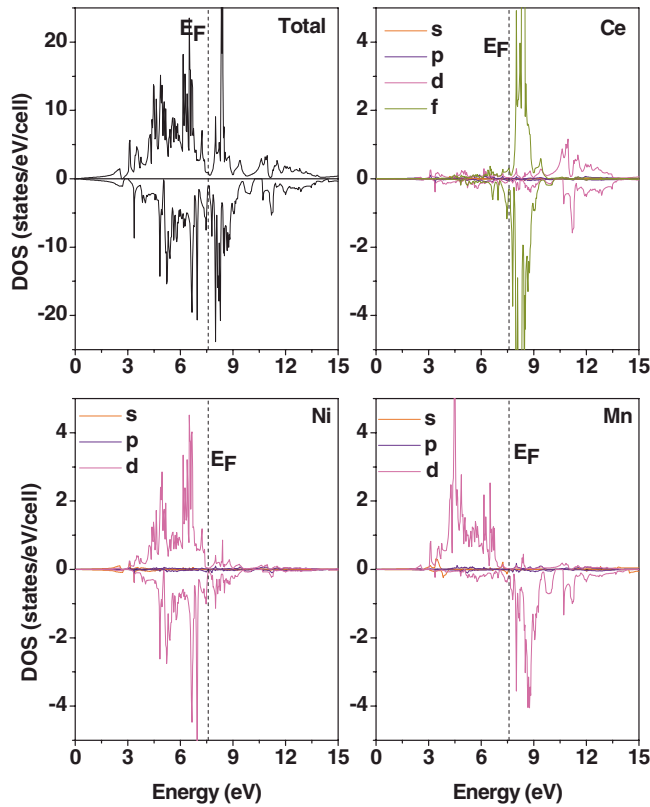


FIG. 4. (Color online) Total and site projected DOS of CeMnNi_4 for ordered (fcc) structure.

change between Mn and Ni atoms lowers the energy for this structure with respect to the original fcc structure by 0.2 eV/f.u. Relaxing this site-exchanged structure further lowers the energy by (0.1 eV/f.u.) and introduces small positional disorder in the system. This clearly demonstrates that single-site exchange is energetically favorable for this compound.²¹ The total and site projected DOS for the site-exchanged configuration is shown in Fig. 5. The total DOS at E_F for down-spin channel increases with respect to the original structure while that for up-spin channel remains the same. From the site projected DOS, Ce 4*f* seems to be more localized and shifted slightly higher in energy with respect to E_F . The site-exchanged Mn 3*d* DOS for down-spin channel increases due to enhanced hybridization with 3*d* states of neighboring Ni atoms which, in turn, modifies down-spin channel of 3*d*-DOS for neighboring Ni atoms. For site-exchanged Ni atom, 3*d* becomes more localized as neighbors are slightly farther from their original position. There is a large decrease in 3*d* bandwidth for this Ni atom and our partial charge analysis indicates that it retains all eight *d* electrons with itself. The enhanced Mn-Ni interaction due to site exchange also induces large change in magnetic moments for both the atoms. The overall magnetic moment of the structure decreases by $0.1\mu_B/\text{f.u.}$ Our calculated static spin polarization, for the single-site-exchanged unrelaxed structure, is -50% which reduces to -47% following relaxation. Hence, our calculations clearly show that the presence of small amount ($\sim 6.5\%$) long-range antisite disorder enhances the static spin polarization in CeMnNi_4 .

The remnant discrepancy with experiment may be due to (i) presence of compositional disorder ($\text{CeNi}_{4+x}\text{Mn}_{1-x}$) in ac-

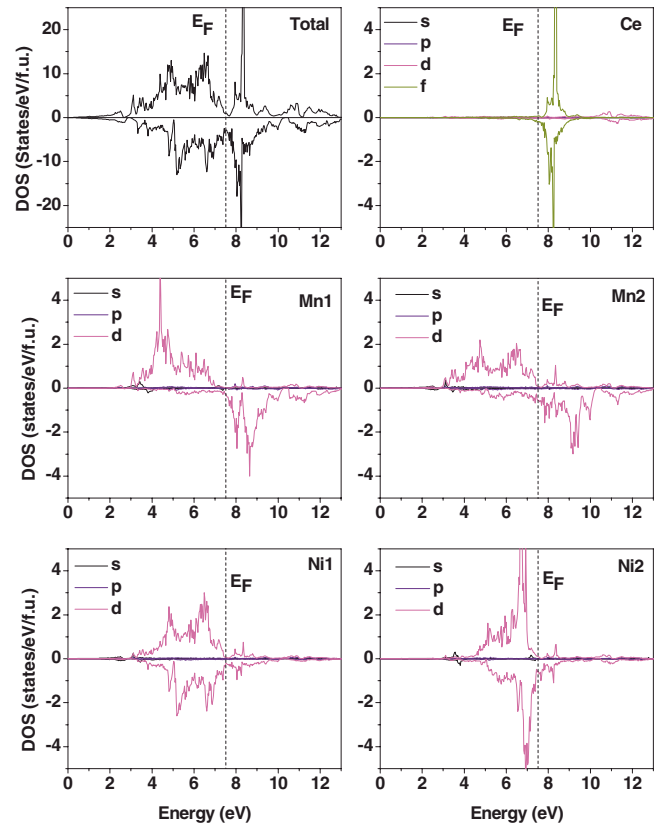


FIG. 5. (Color online) Total and site projected DOS of CeMnNi_4 for site-exchanged structure. (a) Total, (b) Ce, (c) nonsite-exchanged Mn, (d) site-exchanged Mn, (e) nonsite-exchanged Ni, and (f) site exchanged Ni.

tual sample,²² which is out of scope in our calculations or (ii) due to noninclusion of the on-site Coulomb correlation for Mn.²³ The first effect is particularly important because of the different behaviors of the total DOS near Fermi level for the two spin channels. The up-spin channel has a small *pseudogap* near E_F , whereas that for down-spin channel is oscillatory (Fig. 5). Hence, a slight right shift of the Fermi level will cause huge change in polarization. In the rigid-band model, we found from our total DOS that a 0.1 eV right shift of E_F will increase the static spin polarization to -75% . Such a shift of E_F will occur if $\sim 10\%$ Mn is replaced by Ni as each Ni will add three extra valence electrons to the system. On the other hand, the effect of on-site Coulomb correlation (U) has been explored in Ref. 23. Bahramy *et al.*²³ showed that tuning to the value of $U \sim 6$ eV one can get spin polarization very close to the experimental (*Andreev*) value. Our results show that using the experimentally observed abundance of antisite disorder, we obtain a spin polarization $\sim 47\%$ without invoking U . So it is fair to state that 47% polarization is a consequence of (XAFS) experimental results and does not require a large *ad hoc* adjustment of a parameter (i.e., U in Ref. 23) to make the results comparable to the observed value of 66%. Since the correctness of the value of U in Ref. 23 has not been independently deduced, such as from structural or compressibility features of the compound, our results suggest that the U , if present, may be much smaller. Our work and the work of Bahramy *et al.*²³

explore two (complementary) aspects of the problem—the roles of antisite disorder and intrasite correlation energy (U), respectively, in determining the polarization. The difference (between the Andreev polarization and the contribution from antisite disorder) $\sim 19\%$ ($=66\%-47\%$), may be due to the on-site Coulomb interaction. Thus, the relative contribution of antisite disorder and intrasite correlation may be concluded to be $\sim 1.8:1$.²⁴ We would also like to point out that our XAFS results show the largest Debye-Waller factor ($\sigma_{\text{Ni-Mn}}^2 \sim 0.02 \text{ \AA}^2$) for Mn bond (as proposed in Ref. 23). This further confirms the necessity of inclusive consideration of both the approaches. In this context we would like to note that it is also important take into account the difference in the up and down-spin channel Fermi velocities playing a direct role in the spin polarization derived from the Andreev measurements. However, since the up and down Fermi velocities are not very different here, we believe that the qualitative picture will not get altered. Therefore, despite the remnant quantitative discrepancy, the most important aspect of this

work is that disorder antisite disorder in CeMnNi_4 helps enhance the spin polarization significantly.

IV. CONCLUSION

In conclusion, our XAFS results establish $\sim 6\%$ Ni-Mn antisite disorder in CeMnNi_4 , consistent with its low formation energy. Our first-principles calculations demonstrate that this disorder transforms the compound into a half-metal with polarization ($\sim 47\%$) comparable with experimental value ($\sim 66\%$). Sequentially, the site exchange modifies the Mn-Ni and Ni-Ni near neighbor distances or coordination, their degree of hybridization or localization, and subsequently the DOS in a favorable direction. The remnant difference of $\sim 19\%$ may be ascribed to intrasite correlation. This is an instance where antisite disorder is conclusively shown to favor polarization in a system. This work should inspire future studies where disorder could further enhance the polarization toward the ideal value.

*Corresponding author; debduttalahiri@yahoo.com

- ¹S. Das Sarma, J. Fabian, X. Hu, and I. Zutic, *IEEE Trans. Magn.* **36**, 2821 (2000); S. A. Wolf, D. D. Awschalom, R. A. Buhrman, J. M. Daughton, S. von Molnár, M. L. Roukes, A. Y. Chtchelkanova, and D. M. Treger, *Science* **294**, 1488 (2001); H. Ohno, *ibid.* **281**, 951 (1998); S. A. Wolf and D. Treger, *IEEE Trans. Magn.* **36**, 2748 (2000).
- ²G. A. Prinz, *Science* **282**, 1660 (1998); P. J. Brown, K. U. Neumann, P. J. Webster, and K. R. A. Ziebeck, *J. Phys.: Condens. Matter* **12**, 1827 (2000); S. Ishida, S. Fujii, S. Kashiwagi, and S. Asano, *J. Phys. Soc. Jpn.* **64**, 2152 (1995); V. G. Kantser and J. Optoelect, *Adv. Mater.* **8**, 425 (2006); R. Y. Umetsu, K. Kobayashi, R. Kainuma, A. Fujita, K. Fukamichi, K. Ishida, and A. Sakuma, *Appl. Phys. Lett.* **85**, 2011 (2004); I. I. Mazin, *Phys. Rev. Lett.* **83**, 1427 (1999).
- ³S. Kumar and A. P. Kampf, *Phys. Rev. Lett.* **100**, 076406 (2008); I. Galanakis, K. Özdoğan, B. Aktaş, and E. Şaşıoğlu, *Appl. Phys. Lett.* **89**, 042502 (2006); B. Sanyal and O. Eriksson, *Phys. Status Solidi A* **204**, 33 (2007); R. C. Myers, B. L. Sheu, A. W. Jackson, A. C. Gossard, P. Schiffer, N. Samarth, and D. D. Awschalom, *Phys. Rev. B* **74**, 155203 (2006); Z. Chen, S. G. Carter, R. Bratschitsch, P. Dawson, and S. T. Cundiff, *Nat. Phys.* **3**, 265 (2007); S. J. Hashemifar, P. Kratzer, and M. Scheffler, *Phys. Rev. Lett.* **94**, 096402 (2005); P. A. Dowben and R. Skomski, *J. Appl. Phys.* **95**, 7453 (2004); S. R. Eric Yang and A. H. MacDonald, *Phys. Rev. B* **67**, 155202 (2003); M. L. Fdez-Gubieda, A. Garcia-Arribas, J. M. Barandiarán, R. López Antón, I. Orue, P. Gorria, S. Pizzini, and A. Fontaine, *ibid.* **62**, 5746 (2000); C. Song, F. Zeng, Y. X. Shen, K. W. Geng, Y. N. Xie, Z. Y. Wu, and F. Pan, *ibid.* **73**, 172412 (2006); Y. L. Soo, S. Kim, Y. H. Kao, A. J. Blattner, B. W. Wessels, S. Khalid, C. Sanchez Hanke, and C.-C. Kao, *Appl. Phys. Lett.* **84**, 481 (2004).
- ⁴C. Madhu, A. Sundaresan, and C. N. R. Rao, *Phys. Rev. B* **77**, 201306(R) (2008); P. Mahadevan and S. Mahalakshmi, *ibid.* **73**, 153201 (2006); M. Venkatesan, C. B. Fitzgerald, and J. M. D. Coey, *Nature (London)* **430**, 630 (2004).
- ⁵X. J. Wang, I. A. Buyanova, F. Zhao, D. Lagarde, A. Balocchi, X. Marie, C. W. Tu, J. C. Harmand, and W. M. Chen, *Nature Mater.* **8**, 198 (2009).
- ⁶S. Singh, G. Sheet, P. Raychaudhuri, and S. K. Dhar, *Appl. Phys. Lett.* **88**, 022506 (2006).
- ⁷E. N. Voloshina, Y. S. Dedkov, M. Richter, and P. Zahn, *Phys. Rev. B* **73**, 144412 (2006); P. Murugan, A. Kumar Singh, G. P. Das, and Y. Kawazoe, *Appl. Phys. Lett.* **89**, 222502 (2006); I. I. Mazin, *Phys. Rev. B* **73**, 012415 (2006).
- ⁸R. Skomski, *J. Phys.: Condens. Matter* **19**, 315202 (2007); L. M. Sandratskii, *J. Magn. Magn. Mater.* **321**, 924 (2009).
- ⁹S. Picozzi, A. Continenza, and A. J. Freeman, *Phys. Rev. B* **69**, 094423 (2004); Y. Miura, K. Nagao, and M. Shirai, *ibid.* **69**, 144413 (2004); B. Ravel, M. P. Raphael, V. G. Harris, and Q. Huang, *ibid.* **65**, 184431 (2002); M. P. Raphael, B. Ravel, Q. Huang, M. A. Willard, S. F. Cheng, B. N. Das, R. M. Stroud, K. M. Bussmann, J. H. Claassen, and V. G. Harris, *ibid.* **66**, 104429 (2002); B. Ravel, J. O. Cross, M. P. Raphael, V. G. Harris, R. Ramesh, and V. Saraf, *Appl. Phys. Lett.* **81**, 2812 (2002); K. Özdoğan, E. Sasoglu, B. Aktas, and I. Galanakis, *Phys. Rev. B* **74**, 172412 (2006); N. D. Telling, P. S. Keatley, G. van der Laan, R. J. Hicken, E. Arenholz, Y. Sakuraba, M. Oogane, Y. Ando, and T. Miyazaki, *ibid.* **74**, 224439 (2006).
- ¹⁰Except for a few reports, e.g., R. J. Soulen, Jr., J. M. Byers, M. S. Osofsky, B. Nadgorny, T. Ambrose, S. F. Cheng, P. R. Broussard, C. T. Tanaka, J. Nowak, J. S. Moodera, A. Barry, and J. M. D. Coey, *Science* **282**, 85 (1998); B. Nadgorny, I. I. Mazin, M. S. Osofsky, R. J. Soulen, P. Broussard, R. M. Stroud, D. J. Singh, V. G. Harris, A. Arsenov, and Y. Mukovskii, *Phys. Rev. B* **63**, 184433 (2001); R. P. Panguluri, K. C. Ku, T. Wojtowicz, X. Liu, J. K. Furdyna, Y. B. Lyanda-Geller, N. Samarth, and B. Nadgorny, *ibid.* **72**, 054510 (2005); A. Schmehl, V. Vaithyanathan, A. Herrnberger, S. Thiel, C. Richter, M. Liberati, T. Heeg, M. Röckerath, L. Fitting Kourkoutis, S. Mühlbauer, P. Böni, D. A. Muller, Y. Barash, J. Schubert, Y. Idzerda, J. Manhart, and D. G. Schlom, *Nature Mater.* **6**, 882 (2007); A. An-

- guelouch, A. Gupta, G. Xiao, D. W. Abraham, Y. Ji, S. Ingvarsson, and C. L. Chien, *Phys. Rev. B* **64**, 180408 (2001); Y. S. Dedkov, M. Fonine, C. König, U. Rüdiger, G. Güntherod, S. Senz, and D. Hesse, *Appl. Phys. Lett.* **80**, 4181 (2002); G. M. Müller, J. Walowski, M. Djordjevic, G.-X. Miao, A. Gupta, A. V. Ramos, K. Gehrke, V. Moshnyaga, K. Samwer, J. Schmalhorst, A. Thomas, A. Hütten, G. Reiss, J. S. Moodera, and M. Münzenberg, *Nature Mater.* **8**, 56 (2009).
- ¹¹A. Das Indu Dhiman, S. K. Dhar, P. Raychaudhuri, S. Singh, and P. Manfrinetti, *Solid State Commun.* **141**, 160 (2007).
- ¹²R. Prins and D. C. Koningsberger, *X-ray Absorption: Principles, Applications, Techniques of EXAFS, SEXAFS and XANES* (Wiley, New York, 1987).
- ¹³See supplementary material at <http://link.aps.org/supplemental/10.1103/PhysRevB.82.134424> for Andreev results.
- ¹⁴D. Lahiri, *Physica C* **436**, 32 (2006).
- ¹⁵See <http://www.nsls.bnl.gov/beamlines/beamline.asp?blid=X18B>
- ¹⁶M. Newville, B. Ravel, D. Haskel, J. J. Rehr, E. A. Stern, and Y. Yacoby, *Physica B* **208-209**, 154 (1995).
- ¹⁷G. Kresse and J. Furthmüller, *Phys. Rev. B* **54**, 11169 (1996); G. Kresse and J. Hafner, *ibid.* **47**, 558 (1993); G. Kresse and D. Joubert, *ibid.* **59**, 1758 (1999).
- ¹⁸There is no multiple-scattering path contribution over this range.
- ¹⁹In parallel, the data set for each temperature was fit separately to test the fluctuation of the disordered fraction in the sample between temperatures. The result was similar to that from simultaneous fit within uncertainties.
- ²⁰J. P. Perdew, K. Burke, and M. Ernzerhof, *Phys. Rev. Lett.* **77**, 3865 (1996).
- ²¹Double site-exchanged structure is not energetically favorable and spin polarizations reduce to $\sim 32\%$ for this structure.
- ²²For $x \leq 0.1$, the compound is cubic reported by M. Klimczak, E. Talik, J. Kusz, A. Kowalczyk, and T. Tolinski, *Cryst. Res. Technol.* **42**, 1348 (2007).
- ²³M. S. Bahramy, P. Murugan, G. P. Das, and Y. Kawazoe, *Phys. Rev. B* **81**, 165114 (2010).
- ²⁴Polarization (P) without antisite disorder of $\sim 13\%$ and with antisite disorder $P \sim 47\%$. Therefore, contribution of antisite disorder is given by $P_{\text{antisite}} \sim 34\%$. Contribution of intrasite correlation: $P_{\text{intrasite}} \sim 19\%$. Therefore, $P_{\text{antisite}}:P_{\text{intrasite}} = 34:19 = 1.8:1$.